Janez LESKOVEC[1], Makuc DANILO[2], Franci LAHAJNAR[1], Damijan MILJAVEC[2]
Kolektor Group d.o.o. (1), University of Ljubljana (2)

Nonlinear reluctance model of transverse flux motor

***Abstract**. The aim of this paper is to present parametric nonlinear reluctance model of outer rotor permanent magnet transverse flux machine (TFM). Main and leakage magnetic flux paths of TFM are studied and modelled with reluctances using mean length and cross area approximation which divide the model into simple solids. General propose circuit simulator is used to solve the model. The main goal of the model is to provide the results of machine performances with sufficient accuracy and quick enough to use them in optimization procedures.*

***Streszczenie.** Celem artykułu jest prezentacja nieliniowego reluktancyjnego modelu maszyny elektrycznej z poprzecznym strumieniem i z zewnętrznym wirnikiem i magnesem trwałym. Strumienie magnetyczne, główny i rozproszenia, modelowane są z reluktancjami przy użyciu średnich długości i przekrojów, które dzielą model na proste obiekty. Zadaniem symulatora obwodowego jest rozwiązanie modelu. Głównym celem modelowania jest dostarczenie wyników działania maszyny z dostateczną dokładnością i wystarczająco szybko do wykorzystania w procedurach optymalizacyjnych. (**Nieliniowy model reluktancyjny silnika z poprzecznym strumieniem**).*

Keywords: finite element method, nonlinear reluctance model, transverse flux machine
Słowa kluczowe: metoda elementów skończonych, nieliniowy model reluktancyjny, naszyna ze strumieniem poprzecznym

Introduction

The development of soft magnetic composite materials (SMC) increase the interest in electromagnetic structures with 3-D guided magnetic flux, such as transverse flux machine (TFM) [1, 2] shown in Fig. 1. Model of TFM is composed of inner stator made from soft magnetic composite material and outer rotor composed of yoke and permanent magnets. The three phase coils are in form of ring and positioned in the stator slot. The rotor magnets are shifted for 120 electrical degrees circumferentially regarding each phase.

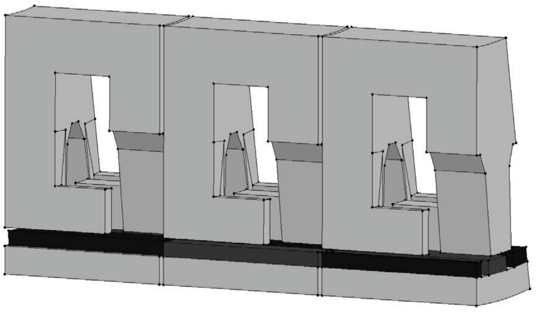

Fig.1. 3-D model of 1/36 transverse flux motor

Further, the paper proposes a parametric nonlinear reluctance model of TFM which provides the results of analysed machine with sufficient accuracy in short period of time. In this way the model can be used in a multi-objective parameters optimization method to provide parameters of the motor geometry which are quite close to optimum values. However, because the magnetic flux leakage and fringing paths in the TFM are spread in all three dimensions the accurate flux paths are hard to define in reluctance model. Regarding these the 3-D FEM analyse of TFM is required to verify the results of reluctance model [3].

Reluctance model of transverse flux machine

The nonlinear reluctance model based on geometric parameters in Table 1, was build for d-axis rotor position (highest magnetically conductive position). The model consists of linear reluctances presenting the air parts (air gap, leakage paths), the nonlinear reluctances for SMC parts, magneto-motive-force source presenting the electric coil and magneto-motive-force sources with internal reluctance acting as permanent magnet.

Only one pole pair and one phase of the TFM can be modelled, because of the periodical symmetry with number of pole pairs and also with assumption that there is no interaction between phases.

First step in building the reluctance model is to select nodes locations which divide the stator, rotor and air parts into simple solids. In this way the flux between two nodes flows just in a uniaxial direction [2].

Proposed nonlinear reluctance model is presented in Fig. 2. Shadowed reluctances are nonlinear and present stator and rotor ferromagnetic parts. The air gap reluctances are (R24-R29) and leakage reluctances are non-shadowed.

The air gap area and leakage flux paths are modelled by linear reluctances in form of equation:

$$R_{\mathrm{air}} = \frac{1}{\mu_0} \cdot \frac{l_{\mathrm{mean}}}{A_{\mathrm{mean}}} \tag{1}$$

where: μ_0 - permeability of free space, l_{mean} - mean length between two nodes, A_{mean} - mean area of cross section [4].

The stator core parts are modelled with nonlinear reluctances:

$$R_{\mathrm{smc}} = \frac{1}{\mu_0 \cdot \mu_{\mathrm{r}}(\phi)} \cdot \frac{l_{\mathrm{mean}}}{A_{\mathrm{mean}}} \tag{2}$$

where: $\mu_r(\phi)$ - relative permeability of material depending on magnetic flux level in reluctance element.

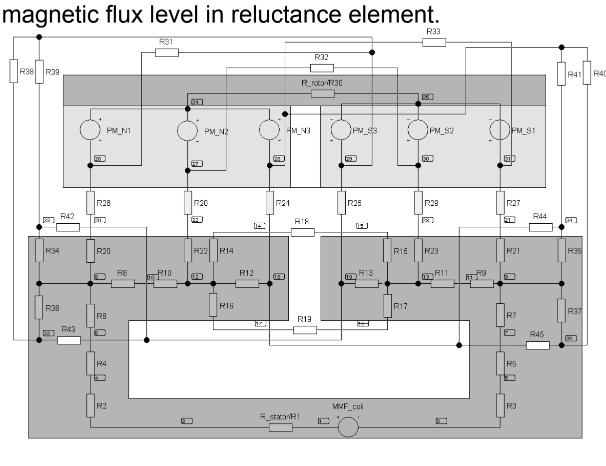

Fig. 2. One pole-pair model of TFM and proposed nonlinear reluctance model.

Permanent magnets are modelled as magneto-motive-source MMF_{mag} with internal reluctance R_{mag}. In form of equation they are expressed as:

(3) $$MMF_{\mathrm{mag}} = H_{\mathrm{c}} \cdot l_{\mathrm{mag}}$$

(4) $$R_{\mathrm{mag}} = \frac{1}{\mu_0 \mu_{\mathrm{r}}} \cdot \frac{l_{\mathrm{mag}}}{A_{\mathrm{mag}}}$$

where: H_c - magnet coercivity, l_{mag} - magnet radial length, A_{mag} - magnet cross section, μ_r - magnet relative permeability.

Table 1. Geometric parameters of the TFM which are modelled.

Geometric parameters	Value
Outer rotor radius (mm)	115
Inner rotor radius (mm)	106.3
Outer stator radius (mm)	105.5
Inner stator radius (mm)	61.5
Axial length of one phase (mm)	37
Radial length of stator yoke (mm)	11
Radial length of stator ring (mm)	22
Axial length of pole tooth (mm)	12
Axial length of pole shoe (mm)	12
Air-gap width (mm)	0.8
Pole pairs (Pp)	36
Angle of pole tooth (mech. deg)	90/Pp
Angle of pole shoe (mech. deg)	150/Pp
Angle of pole shoe in the middle (mech. deg)	210/Pp
Angle of pole shoe at bottom (mech. deg)	300/Pp
Radial magnet length (mm)	3
Angle of magnet width (mech. deg)	127.5/Pp
Stator slot dimensions (mm x mm)	13 x 20
Number of turns per phase	13

TFM performance calculation using nonlinear reluctance model

The nonlinear reluctance model in form of magnetic equivalent circuit (MEC) is created and solved using general purpose circuit simulator (Pspice). Magnetic flux flowing through each element of reluctance model is calculated based on MEC. Further, the magnetic flux density in each reluctance element is calculated. Assuming the sinusoidal time dependant magnetic flux distribution through stator winding the no-load amplitude of inducted voltage can be expressed [4, 5, 6, 7, 8, 12]:

(6) $$E_{\mathrm{f}} = 2\pi\, f_{\mathrm{mech}}\, N_1\, P_{\mathrm{P}}^{\,2}\, \phi$$

where: N_1 - number of stator turns per phase, f_{mech} - mechanic frequency of rotation, P_p - number of pole pairs, ϕ - peak value of excitation magnetic flux without armature reaction.

When motor is fed by the current in phase with induced voltage E_f (no-load voltage) the electromagnetic power P_{em} and electromagnetic torque T_{em} can be calculated:

(7) $$P_{\mathrm{em}} = m \frac{1}{2} E_{\mathrm{f}}\, I_{\mathrm{q}}$$

(8) $$T_{\mathrm{em}} = \frac{P_{\mathrm{em}}}{\omega_{\mathrm{mech}}}$$

where: m - number of phases in our case $m=3$, Iq - amplitude value of imposed current in phase with induced no-load voltage, E_f - amplitude value of inducted no-load voltage, ω_{mech} - mechanical speed of rotation.

Since the magnetic flux density for each reluctance element is known the ferromagnetic losses in whole TFM can be calculated. Measured core losses of Somaloy 700 [10] are used to determine the function (9) coefficient k_e (eddy current coefficient) and k_h (hysteresis losses coefficient) with least mean square method.

(9) $$P_{smc} = \left(k_e \cdot f^2 + k_h \cdot f\right) \cdot B^2 \cdot m_{smc}$$

where: P_{smc} – Ferromagnetic losses in reluctance element, k_e – eddy current coefficient, k_h - hysteresis losses coefficient, f – electrical frequency, B - magnetic flux density in reluctance element, m_{smc} – weight of solid representing reluctance.

Table 2. Core losses for Somaloy 700 at B=1T.

Frequency (Hz)	Core losses at 1T (W/kg)
50	5
200	22
400	48
600	79
800	111
1000	147

Based on equation (9) and measured core losses at different frequencies, as shown in Table 2, the coefficients are obtained:

(10) $$\begin{aligned} k_{\mathrm{e}} &= 3.846e-5 \quad \mathrm{Ws^2}/\left(\mathrm{T^2 kg}\right) \\ k_{\mathrm{h}} &= 0.09953 \quad \mathrm{Ws}/\left(\mathrm{T^2 kg}\right) \end{aligned}$$

For SMC material is considered that eddy current loss can be neglected since every iron particle is electrical isolated and therefore the material electrical resistance is very high [9, 10, 12].

The total core losses of the TFM are the sum of all losses in all modelled ferromagnetic reluctances considering the number of pole-pairs and the number of phases.

Cooper loss can be calculated using:

(11) $$P_{\mathrm{cu}} = \frac{m}{2} I^2 R$$

where: I - amplitude of phase current, R - winding resistance, m - number of stator phases.

The efficiency η of analysed TFMs is expressed as:

(12) $$\eta = \frac{P_{\mathrm{em}} - \left(P_{\mathrm{smc}} + P_{\mathrm{cu}} + P_{\mathrm{fric\_wind}}\right)}{P_{\mathrm{em}}} = \frac{P_{\mathrm{mech}}}{P_{\mathrm{em}}}$$

where: P_{fric_wind} - friction and windage losses, P_{smc} - iron losses in ferromagnetic parts of the TFM.

Verification of nonlinear reluctance model

The results obtained by the nonlinear reluctance model, 3-D FEM model and measurement results done on prototype all with the same geometrical parameters, as in Table 1 are compared in Table 3. The working point for all analyses and measurements was set to mechanical speed at 70 rpm and with an imposed phase current amplitude of 50 A. The mechanical torque for nonlinear reluctance model is calculated by equation (8) using mechanical power derived in equation (12).

The proposed model has also been compared with 3-D FEM model with variation of pole-pairs from 15 to 36.

Magnetic fluxes in stator and rotor at magnetically aligned position are compared in Fig. 3 for both models. Reluctance model overestimate flux through stator and underestimate flux through rotor. Stator and rotor flux error of a proposed model are inside the range of 15% over whole region of varied pole pairs. The results are presented in Fig. 4.

Table 3. The comparison of results at 70rpm and phase current amplitude 50A for 36 pole-pairs TFM design

TFM	EMF amplitude (V)	Electromagnetic Torque (Nm)	Mechanical Torque (Nm)
Nonlinear reluctance model	12.09	123.7	112.5
FEM model	11.7	96.3	
Measurement at TFM prototype	11.9		90

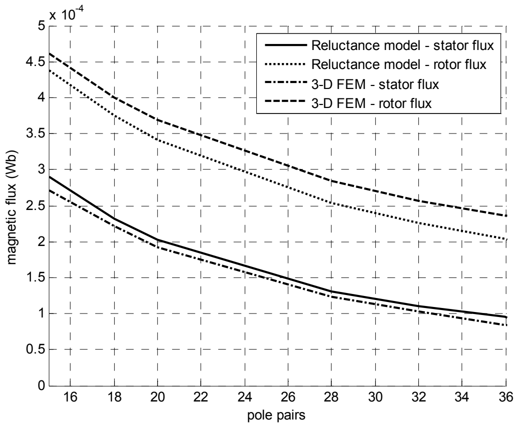

Fig. 3. Nonlinear reluctance model and 3-D FEM model stator and rotor magnetic flux comparison.

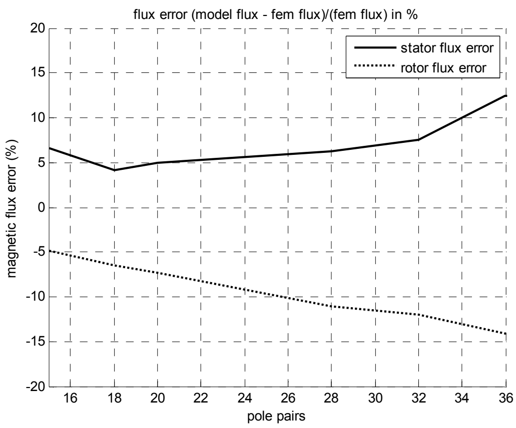

Fig. 4. Nonlinear reluctance model stator and rotor magnetic flux error compared to 3-D FEM flux in percentage.

The inducted voltages for both models are compared in Fig. 5. The results of electromagnetic torques and mechanical torque at phase current amplitude 50A for varied pole pairs are compared in Fig. 6. Table 3 and Fig. 5 show good agreement between amplitudes of no-load inducted phase voltages for all compared models regarding reluctance models and FEM models and also in comparison with measurement on TFM prototype. On the other hand torque comparison shows higher difference that can be expected from no-load inducted voltage for proposed model.

Therefore no-load inducted phase voltages calculated by 3-D FEM model (prototype based) and measured results of prototype (36 pole-pairs TFM design) at mechanical speed of 70 rpm were further investigated. No-load inducted three phase voltages calculated by 3-D FEM model are presented in Fig. 7 in time and frequency domain which were obtained from Fourier transform.

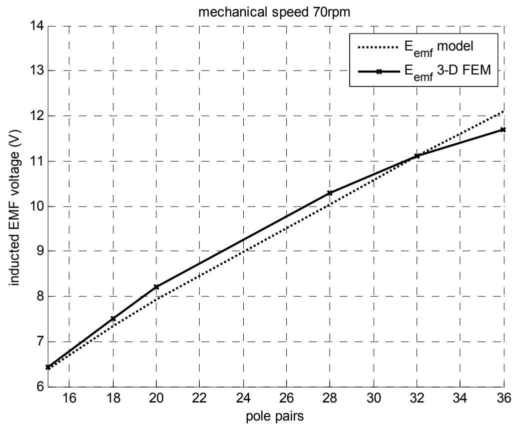

Fig. 5. No-load inducted phase voltage amplitude of nonlinear reluctance model and 3-D FEM model

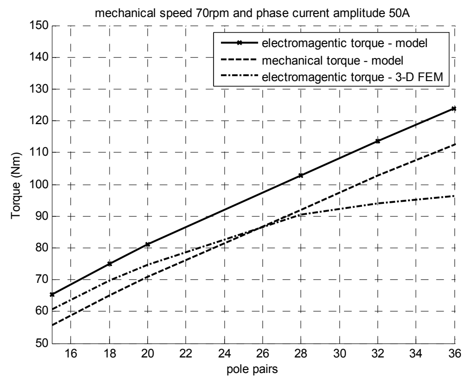

Fig. 6. Electromagnetic and mechanical torque at current amplitude 50A for nonlinear reluctance model an 3-D FEM model

The same analyses were done for measured no-load inducted phase voltages of prototype and results are presented in Fig. 8. From frequency domain of both sets of inducted voltages it can be seen that there is also a third harmonic component present, which do not contribute to the shaft torque [11]. On the other hand, measured first harmonic phase voltage is lower than calculated one. Meanwhile, the amplitude values of no-load inducted voltage show very small differences between calculated and measured values (Table 3). From the fact that we suppose in reluctance model that the induced phase voltage is composed just of first harmonic component the main differences in torque calculation arise. Not taking into account the third harmonic component of induced phase voltage overestimate the torque capabilities of analyzed TFM designs

It can be seen that proposed model, because of its nonlinear reluctances, predicts the peak value of magnetic flux through stator winding and therefore the amplitude of inducted voltage with sufficient accuracy (Fig. 5). Because only d-axis rotor position is modelled and the assumption of sinusoidal time dependant magnetic flux distribution through stator winding is used the model can not predict the higher harmonics in inducted voltage (time dependant induced voltage) and therefore the electromagnetic torque could be overestimated. The saturation of ferromagnetic parts of modelled TFMs and leakage fluxes are taken into account in reluctance model and are integrated in the amplitude value of induced no-load phase voltage.

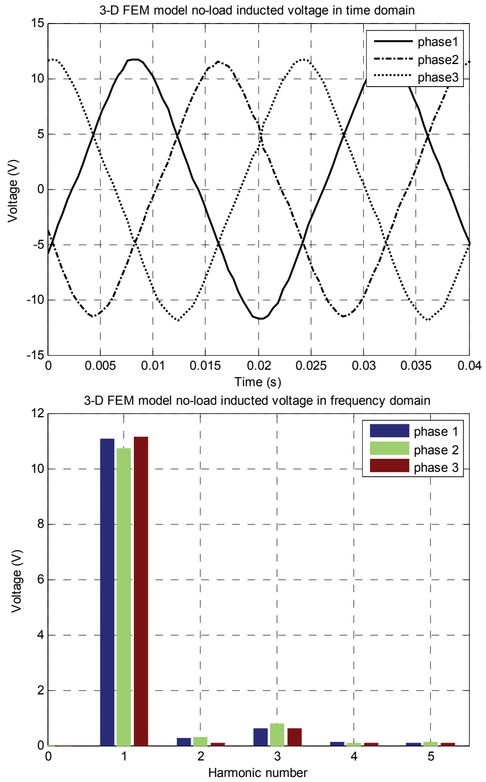

Fig. 7. 3-D FEM model no-load inducted voltage in time and frequency domain at 70rpm.

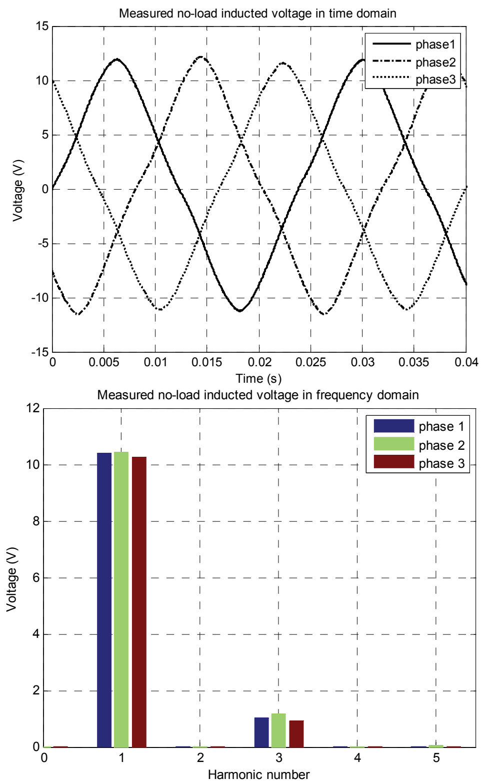

Fig. 8. Measured no-load inducted voltage in time and frequency domain at 70rpm.

Conclusion

In the process of a transverse flux machine design optimization the use of 3-D finite element (FEM) is almost obligatory to get sufficient accuracy. The main problem using 3-D FEM is the time consuming calculation. Proposed nonlinear reluctance model gets fast and accurate enough results of TFM performance. The model can be used in multi-objective parameter optimization methods to provide initial values of TFM geometric parameters which are close to required and optimum values. These values define the starting design for further verification and optimization in 3-D finite element analyses.

In the presented reluctance nonlinear model only d-axis rotor position is modelled and the assumption of sinusoidal time dependant magnetic flux distribution through stator winding is made. So defined model can not predict the higher harmonics in inducted voltage and therefore the electromagnetic torque could be overestimated. In the further work, the presented nonlinear model will be improved with ability to calculate the space dependant high harmonics components of induced phase voltage.

REFERENCES

[1] A. Masmoudi, A. Njeh, A. Mansouri, H. Trabelsi, A. Elantably, "*Optimizing the overlap Between the Stator Teeth of a Claw Pole Transverse-Flux permanent-Magnet Machine*", IEEE Transactions on Magnetics, vol. 40, no. 3, pp. 1573-1578, May 2004.

[2] W. M. Arshad, T. Bäckström, C. Sadarangani, "*Analytical Design and Analysis Procedure for a Transverse Flux Machine*", Royal Institute of Technology, Proceedings of the IEEE International Electrical Machines & Drives Conference (IEMDC), Boston, June 2001.

[3] Y.G. Guo, J.G. Zhu "*Study of Permanent Magnet Transverse Flux Motors with Soft Magnetic Composite Core*", AUPEC 2004, Brisbane, Australia.

[4] J. F. Gieras, M.Wing "*Permanent Magnet Motor Technology*", New York: Marcel Dekker, 2002.

[5] L. Gašperlin, A. Černigoj, S. Markoč, R. Fišer, "*Additional cogging torque components in permanent-magnet motors due to manufacturing imperfections*", IEEE trans. magn., vol. 45, no. 3, pp. 1210-1213, Mar. 2009.

[6] M. Nemec, D. Nedeljković, V. Ambrožič, "*Predictive torque control of induction machines using immediate flux control*". IEEE trans. ind. electron., vol. 54, no. 4, pp. 2009-2017, Aug. 2007.

[7] P. Virtič, P. Pišek, M. Hadžiselimović, T. Marčič, B. Štumberger, "Torque analysis of an axial flux permanent magnet synchronous machine by using analytical magnetic field calculation". *IEEE trans. magn.*, vol. 45, no. 3, pp. 1036-1039 Mar. 2009.

[8] P. Anpalaham, "*Design of transverse flux machines using analytical calculations & finite element analysis*", Tech. Licentiate Thesis, Royal Institute of Technology, Stockholm, 2001.

[9] Lars H. O. Andersson, "*Advances in SMC Technology – Materials and Applications*", EURO PM2009 Copenhagen, Denmark.

[10] "*Somaloy Prototyping Material Brochures*", Höganäs AB, Höganäs Sweden.

[11] G. Venkatesan, R. Arumugam, S. Paramasivam, M. Vasudevan, S, Vijayan, "*Occurrence of Harmonics with Induction Machine and Switched Relucatance Machine: A Survey and Analysis*", Journal of Applied Science 6(9), 2126-2130, 2006, ISBN 1812-5654.

[12] P. Anpalaham, "*Design of transverse flux machines using analytical calculations & finite element analysis*", Tech. Licentiate Thesis, Royal Institute of Technology, Stockholm, 2001.

***Authors**: Janez Leskovec, Kolektor Group d.o.o., Vojkova 10, 5280 Idrija, Slovenia, E-mail: janez.leskovec@kolektor.com; M.Sc. Makuc Danilo, University of Ljubljana, Faculty of Electrical Engineering, Trzaska 25, 1000 Ljubljana, Slovenia, E-mail: makuc.danilo@fe.uni-lj.si; Ph.D. Franci Lahajnar, Kolektor Group d.o.o., Vojkova 10, 5280 Idrija, Slovenia, E-mail: franci.lahajnar@kolektor.com; prof. Ph.D. Damijan Miljavec, University of Ljubljana, Faculty of Electrical Engineering, Trzaska 25, 1000 Ljubljana, Slovenia, E-mail: miljavec@fe.uni-lj.si.*